Hindawi
International Journal of Chemical Engineering
Volume 2022, Article ID 5443317, 10 pages
https://doi.org/10.1155/2022/5443317

Research Article

Crude Oil Foulant Deposition Studies on a Heated Surface Using a Novel Batch Stirred Coupon Test Rig

Pragya Singh,[1] Srinivas Krishnaswamy ,[1] Krishnaswamy Ponnani,[1,2] Ankur Verma,[3] and Jaya Rawat[3]

[1]*Centre of Excellence in Process Engineering & Intensification (COE-PE&I), Department of Chemical Engineering, BITS–Pilani, K K Birla Goa Campus, Zuarinagar, Goa, India*
[2]*E2DStech, Present Address: 15/151 (Old 7/383) Sreenivas,Sivan Kovil Street, Tharakkad, Palakkad, Kerala 678001, India*
[3]*Bharat Petroleum Corporation Limited Corporate R&D Center, Corporate R&D Center, Greater Noida, India*

Correspondence should be addressed to Srinivas Krishnaswamy; srinivas@goa.bits-pilani.ac.in

Received 3 February 2022; Revised 24 April 2022; Accepted 28 April 2022; Published 26 May 2022

Academic Editor: Ho SoonMin

The petroleum refining industry employs a wide variety of heat transfer-based equipment which tend to foul due to the complex nature of associated fluid streams and process conditions. Over the years, different test methods have been researched to understand fouling at the lab, pilot, and/or plant level. Several of these investigations have been limited to understanding fouling in static refinery streams or under non-practical operating conditions. The present study experimentally demonstrates the potential of a high-temperature batch stirred coupon test rig to characterize fouling under noncoking conditions for a specific refinery stream of interest. Experiments were conducted using a representative crude oil stream (obtained from a refinery) in a 2-liter batch autoclave system with a facility to immerse coupons attached to a rotating shaft into the stream during related test runs. The coupon Material of Construction (MOC) was chosen similar to the MOC of the tubes used in a refinery crude heat exchanger train. Experiments covered a range of bulk temperatures from 250°C to 300°C at 100 RPM. The foulant deposits obtained were found to have a strong (hard) and weakly (soft) adhering component. In the temperature range investigated, the hard and soft deposits were largely inorganic and organic in nature, respectively. The fluid bulk temperature was found to influence hard and soft deposit formation. The foulant deposits were characterized using TGA, CHNS, XRD, and SEM/EDAX, respectively. The iron and sulfur content in the hard deposit was more than 45% in total, indicating that the fouling mechanism was corrosion-based resulting from the formation of FeS on the surface. The thermal history of the soft deposit was distinct from the crude oil used. The results obtained confirm the potential of the coupon test rig for understanding fouling in refinery streams.

1. Introduction

Petroleum or crude oil refining has long been the primary backbone for meeting global energy demands, producing fuels that have been used in industry, transportation, and homes. Fouling has been identified as a major cause of sub-optimal operation in refinery systems leading to plant downtime and production loss [1, 2]. This occurs as a result of increased thermal resistance caused by the deposition of unwanted organic and/or inorganic materials present in a petroleum stream when flowing over surfaces of processing equipment [3, 4]. More than 3% reduction in refinery operational efficiency and revenue can be attributed to fouling in such equipment, particularly at higher temperatures. Furthermore, the environmental impact due to fouling in refineries accounts for significant emissions of carbon dioxide (CO_2) [5, 6]. Any attempt to mitigate fouling will help address this dual problem of energy and the environment simultaneously.

Many fouling mechanisms have been identified to occur in refinery equipment, which include crystallization, corrosion, chemical reaction, and particulate deposition. These mechanisms act individually or in combination with each other [7]. Several theoretical and experimental studies to

Table 1: Summary of important experimental investigations conducted on fouling.

Test facility	Test fluid	T_{bi} (°C)	T_{bo} (°C)	T_w (°C)
Continuous flow system [17]	Crude oil	130	220	300
Batch autoclave [23]	10% Indene in kerosene	82	—	188
Continuous flow loop system [24]	Crude oil	70–85	—	100–125
Continuous hot liquid process simulator (HLPS) [25]	Light crude oil	65	—	250–400
Batch stirred cell system [26]	Crude oil blends	240–280	—	345–420
Pilot-scale parallel tube apparatus [27]	Maya crude oil	150	—	250–280
Continuous flow loop system with recirculation [1]	Crude oil and heavy oil blends	85	—	220–370
Continuous high-temperature fouling unit [28]	Crude oils	40–300	—	114–515
High-pressure crude oil fouling rig [29]	Nonfouling oil	<100	—	–
Continuous bench-type fouling test rig [30]	Crude oils and blends	—	—	393

date have attempted to better understand these complex mechanisms. One approach involves characterizing oils under static conditions and evaluating fouling propensity based on stream incompatibility and concentration of saturates, aromatics, resins, and asphaltenes [8–16]. This is, however, of little interest in refineries where the unit processes and operations involved are dynamic in nature. Fouling is also dependent on factors such as temperature, flow velocity, time, and equipment surface characteristics. The emphasis should therefore be on predicting fouling under dynamic conditions, utilizing the most advanced test rigs to generate foulant deposits for characterization, and eventually extrapolating this information to systems in practice. Laboratory test setups have been developed for this purpose. Some of the major approaches in the design of such setups have been patented [17–22]. Table 1 presents a summary of significant experimental investigations conducted over the years with the associated fluids used and operating temperatures.

These studies were mainly concerned with examining the impact of fouling on heat transfer on tubular test surfaces. However, these investigations are limited by the constraints imposed by

(i) Accelerated fouling promoted by electrical heating, resulting in nonuniform surface temperatures [26]

(ii) Nonpractical temperature differences between the test surface and fluid [1, 24–27, 29]

(iii) Use of test fluids that are distinct from crude and heavy oils [23, 29]

(iv) High sample requirement [17]

(v) Cumbersome experimental protocols [26, 28, 31]

Attempts have also been made to characterize foulant deposits in some of these studies [26, 31–39]. However, the deposits characterized were those that adhered nonuniformly to heated surfaces under varying operating conditions. Deposit characterization has also been based on the flow of multiple streams of different nature over surfaces, especially when such studies were carried out in systems encountered in practice [32].

Fouling mechanisms can be better understood by testing a specific stream of interest under fixed operating conditions. The know-how can then be applied to study heat transfer on surfaces that foul when exposed to changing

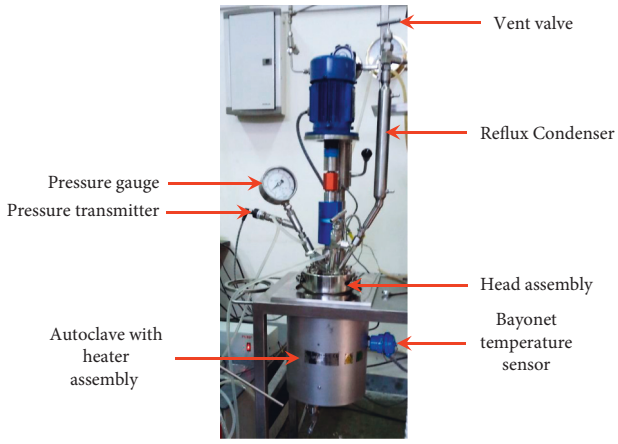

Figure 1: Photograph of the test rig.

temperatures and fluid velocities. This formed the genesis of the present work which aims to demonstrate the potential of a novel batch coupon test rig with an autoclave in predicting fouling under dynamic flow conditions.

The autoclave design was based on an approach adopted by Wang and Watkinson [31, 40, 41] who studied fouling on a cylindrical surface immersed in a rotating fluid maintained at a constant temperature. The coupons represent differential surface elements of fouling heat transfer surfaces at constant temperature and near-uniform shear stress [42]. The rig facilitates easy removal of deposits for further analysis and characterization. This work emphasizes on relating inorganic foulant deposition on a surface to the easily measurable fluid bulk temperature as against the surface temperature, which has been the focus in past investigations, but is never monitored in practice. The temperature range chosen for this study corresponds to the conditions under which corrosion fouling has been widely observed in refinery systems. Details of the rig, experiments performed, and results are presented herewith.

2. Materials and Methods

2.1. Experimental Test Rig. A photograph of the assembled test rig is shown in Figure 1. The 2-liter autoclave (120 mm ID and 300 mm height) was made of SS-316L and surrounded by a 2.5 kW ceramic band heater (127 mm ID and 260 mm height) fitted with a cascade controller. The

controller was driven by a temperature sensor that measured the outer surface temperature of the autoclave. This temperature, based on trial run investigations, was always maintained at a set value above the bulk temperature of the fluid inside the autoclave. This difference was on average around 35°C and facilitated maintaining the fluid temperature at the desired value. The autoclave and heater assembly were insulated using glass wool to prevent heat loss. A head assembly was used to close the system when in operation.

A Bourdon pressure gauge attached to this assembly (WIKA make, range: 0–100 bar, accuracy: ±1.0% of full scale) was used to measure the inside pressure of the autoclave. The pressure was also recorded using a WIKA make pressure transmitter (range: 0–150 bar, accuracy: ±0.5% of full scale). Cooling water was circulated through a jacket enclosing the pressure gauge and pressure transmitter to avoid overheating these systems. A reflux condenser was used to condense any low boiling vapors arising from the sample during the test runs, which were directed back into the autoclave by gravity. A vent valve at the outlet of the condenser in a closed position helped maintain the system pressure and prevent the release of any vapor into the atmosphere during experimentation. The same valve was opened and used to depressurize the system at the end of every run. The autoclave was designed to operate below pressure and temperature of 100 bar (g) and 500°C, respectively. The fluid temperature was measured using two Nickel-chromium/Nickel-aluminum (K−type) thermocouples positioned at a distance of 135 mm and 290 mm from the head assembly. A flush bottom valve provided at the bottom of the autoclave was used to discard the sample after each experimental run.

The coupons used for experimentation were made of carbon steel (AISI 1060) with dimensions of 7.5 cm (length) × 1.2 cm (breath) × 0.1 cm (thickness). These coupons were positioned vertically at two prescribed levels on a solid central shaft (290 mm in height) mounted on the head assembly. At a particular level, the coupons were anchored between two adjustable circular discs using ceramic washers and screws. A maximum of 6 coupons (at 60° positions on a disc) could be anchored at a particular level. In all, a maximum of 12 coupons could be accommodated across the two levels.

A clamp was used to hold the shaft in place, thereby eliminating vibration of the shaft while rotating at RPM values greater than 500. The shaft rotation could be varied up to a maximum of 1400 RPM. A detachable agitator at the lower end of the shaft prevented the formation of dead zones at the autoclave bottom and ensured sufficient mixing of the sample mass. Figures 2(a) and 2(b) show photographs of a test coupon and a set of coupons anchored to the shaft along with the agitator, respectively.

The central shaft was rotated using a magnetic drive unit comprising two interconnected magnets arranged concentrically. While the inner magnet was connected to the shaft, the outer magnet was coupled to an electric motor (1/4 HP, AC supply) mounted on a support plate through a torque sensor (0–10 N–m). A SCADA-based Data Acquisition System (AMAR DAS 4.0) provided by Amar Equipment Pvt. Ltd. (Mumbai, India) was used to record data. The product gases from the autoclave were safely released into the atmosphere through the outlet of the condenser before opening the reactor system at the end of each test run.

2.2. Experimental Method. Prior to the start of a run, all coupons were polished using sandpaper (Grit size: 180) to remove surface flaws, if any, and washed with distilled water and acetone. After cleaning, these coupons were dried at room temperature and their surface roughness was measured using a portable surface roughness tester (Surftest SJ-410 Series, Mitutoyo make, Japan).

The coupons were independently weighed using an analytical balance (Shimadzu make, accuracy: 0.1 mg) and mounted on the shaft using the anchoring arrangement discussed in Section 2.1. The autoclave was filled with approximately 1.8 liters of crude oil and closed by bolting the head assembly. The motor was coupled to the shaft via the magnetic drive and locked into position. With the vent valve at the reflux condenser outlet closed, the system was pressurized to 30 bar (g) with nitrogen and leak tested for 2 hours to assess the integrity of the test rig. The system was then depressurized to ~8 bar (g).

The fluid was heated to attain the desired bulk temperature of 250°C at 100 RPM. The two thermocouples used to measure the bulk temperature were within 1°C of each other under these conditions. Tests showed that no significant deposition occurred during this heating process. The system was allowed to operate for 80 hours following which the heater was switched off and the fluid cooled to ~120°C without agitation. The system was then depressurized to atmospheric pressure using the vent valve.

The head assembly along with coupons attached to the shaft was thereafter unbolted from the autoclave and kept on a custom-designed side seat for 8 hours. This enabled cooling of the assembly to room temperature and gravity draining of the test fluid which would have adhered to the coupons during removal. Each coupon with accumulated foulant deposits was detached from the shaft, washed using 100 ml of n-heptane as a solvent, dried for 1 hour at room temperature, and weighed. Deposits washed away with n-heptane were collected in a Petri dish. The Petri dish and its contents were placed in an oven for 8 hours, maintained at 100°C to evaporate the solvent, and its weight was subsequently noted. The above protocol was repeated at 275 and 300°C at the same agitation speed with the test fluid sample taken afresh in each experiment.

The relatively long experimentation time and limited availability of test samples posed a constraint on repeating experiments using a single coupon under the same operating conditions. Results from multiple coupons immersed in the autoclave fluid during a particular test run were therefore used to confirm the consistency of the results.

3. Results and Discussion

3.1. Nature of Deposits. Fouling was promoted on the surface of 12 coupons immersed in a crude oil sample provided by BPCL Corporate R&D Center. The important properties of

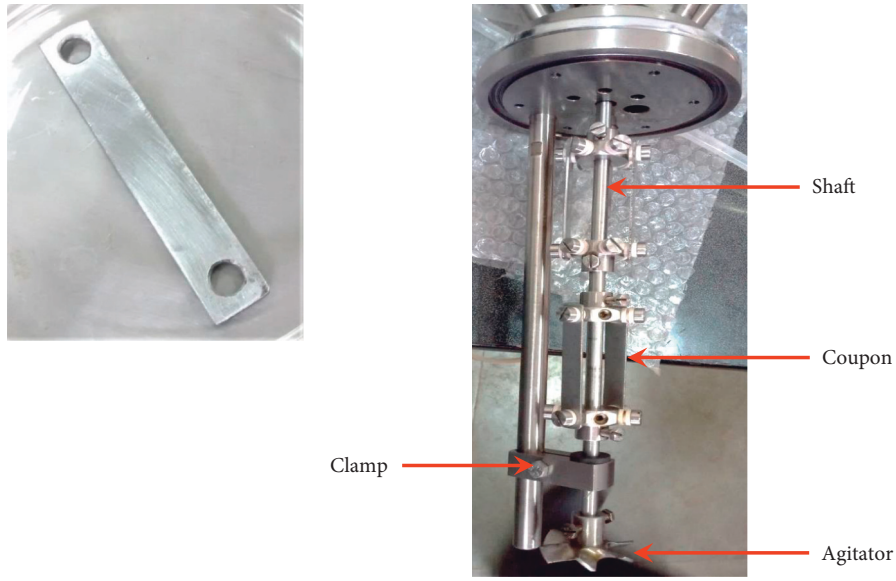

Figure 2: (a) Test coupon. (b) Photograph of the shaft, coupon assembly, and agitator (only 2 coupons shown attached at each level).

the oil are listed in Table 2. As mentioned in Section 2.2, each coupon was removed and washed independently with n-heptane. A part of the foulant deposits formed was found to be carried away by n-heptane, while a portion remained strongly adhered to the coupon surface and could only be removed by scraping. These are henceforth referred to as soft and hard deposits, respectively. Figures 3(a) and 3(b) show hard deposits (HD) accumulated on a coupon and collected after scraping. The soft deposit (SD) in n-heptane and after drying is shown in Figures 4(a) and 4(b), respectively.

3.2. Characterization of Hard Deposits. Hard deposits were collected from two separate test runs carried out at 275 and 300°C for a duration of 80 hours. These deposits were scraped from both surfaces of each coupon using a stainless steel scalpel and cumulatively collected. Sufficient care was taken during scraping to ensure that the coupons were not damaged during the process (confirmed by measurement of surface roughness prior to the commencement of the next run). The deposits were characterized using TGA, CHNS, XRD, and SEM/EDAX. The characterization protocol adopted was based on an analysis philosophy suggested by Brons et al. [43] and summarized by Chew et al. [44]. The sequence of analyses involved two levels as illustrated in Figure 5.

Thermogravimetric analysis (TGA) was used to estimate the relative quantities of volatile/combustible (organic) and nonvolatile (inorganic) components in the hard deposits. Tests were performed using a TGA–DSC (Make: TA Instruments (Waters), Model: Discovery SDT 650). Approximately 9 mg of HD sample was first heated in a nitrogen environment from 30°C to a final temperature of 800°C at a scanning rate of 10°C/min and subsequently combusted in the air for 20 minutes at 800°C. These parameters were selected on the basis of trial runs and information provided in the literature [44].

Table 2: Properties of sample 1.

Element	Result
API	30.87
Viscosity (cP) @ 38°C	2.631
Viscosity (cP) @ 200°C	0.843
C (wt. %)	84.72
H (wt. %)	12.43
N (wt. %)	1.93
S (wt. %)	1.83
Saturates (wt. %)	25.58
Aromatics (wt. %)	44.38
Resins (wt. %)	27.37
C_7 asphaltenes* (wt. %)	1.76
CII	0.38
Fe (ppm)**	2.31
Mg (ppm)**	1.26
Na (ppm)**	7.16
Ni (ppm)**	6.95
Si (ppm)**	86.54
V (ppm)**	17.7

*Estimated using ASTM D 6560 protocol. **Elemental analysis done using ICP-AES.

Table 3 shows the weight percentage of volatiles, combustibles, and ash in the deposits collected at 275°C and 300°C at 100 RPM. The organic content is found to increase with temperature. The high percentage of ash confirms the deposits to be predominantly inorganic in nature.

The sulfur content in the deposits was estimated using a CHNS analyzer (Thermo Scientific make, Model FLASH 2000). This analysis also helped quantify the content of carbon (C), hydrogen (H), and nitrogen (N) in the deposits. The results are tabulated in Table 4.

The results indicate a relatively high content of sulfur in the deposit samples (~30% and above). The hydrogen to carbon ratio was found to be 1.73 and 1.93 at 275 and 300°C,

(a) (b)

Figure 3: (a) Hard deposit on the coupon before scraping. (b) Hard deposit after scraping (obtained at 275°C, 100 RPM, after 80 hours of test run).

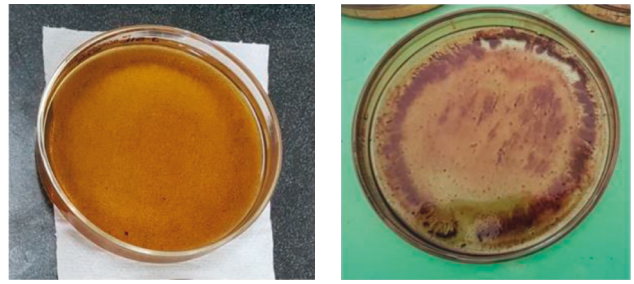

(a) (b)

Figure 4: (a) Soft deposit in n-heptane. (b) Soft deposit after drying (obtained at 275°C, 100 RPM, after 80 hours of test run).

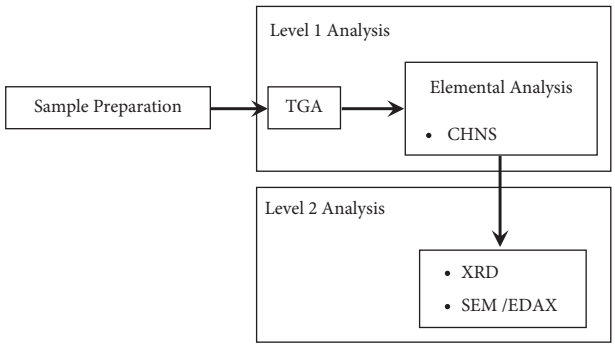

Figure 5: Fouling deposit analysis sequence.

Table 3: TGA results for hard deposits.

Components	Hard deposit composition (wt. %)	
	275°C	300°C
Volatiles	8.2	9.6
Combustibles	7.5	11.3
Ash	84.3	79.1

respectively. These H/C values indicate that the organic content in the deposit at the two temperatures investigated has degraded less with time to form coke-like material [44].

The XRD spectrum of hard deposit samples at the two temperatures is shown in Figure 6. The analysis was done for 2θ values from 10 to 80° using an X-Ray Diffractometer (Model: Bruker D8 Advance).

Table 4: CHNS Analysis data for hard deposits.

Elements	Composition (wt. %) (275°C, 100 RPM)	Composition (wt. %) (300°C, 100 RPM)
C	7.84	8.89
H	1.13	1.43
N	0.01	0.04
S	32.34	29.78

The spectra show characteristic peaks of iron sulfide and iron oxide at both temperatures. The peak intensities confirm the deposit samples to mainly contain iron sulfide compared to iron oxide. The XRD pattern at 300°C shows a dominant peak of sulfur at a 2-theta position of 27.32° [45]. The presence of sulfur in refinery deposits has been reported in the literature [38]. The crystallite size of FeS was calculated using the Scherrer equation and estimated to be 40.92 nm and 85.93 nm at 275 and 300°C, respectively. The crystallite size of iron oxide was also found to increase with temperature and was estimated to be 7.70 nm at 275°C and 15.98 nm at 300°C. The relative crystallite sizes obtained confirm the formation of FeS to dominate the formation of iron oxide at the respective temperatures.

3.3. Characterization of Soft Deposits. The soft deposit collected was also analyzed using a TGA. Figure 7 shows the thermal behavior of soft deposits collected at 300°C and 100 RPM.

The soft deposit is largely organic in nature with the composition of volatiles and combustibles being more than

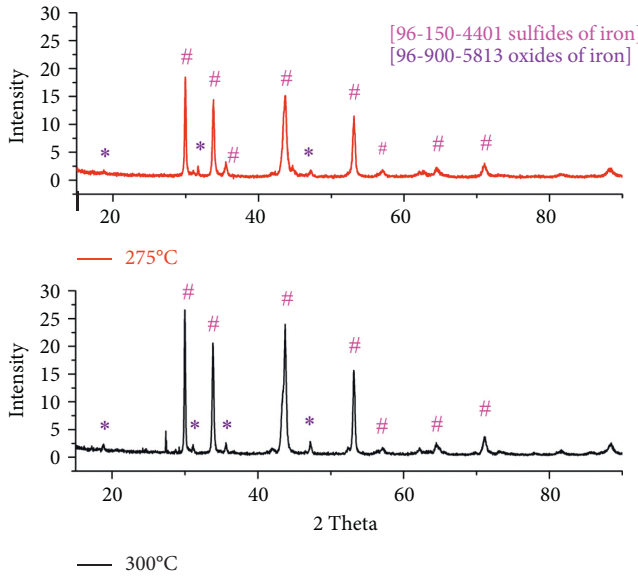

Figure 6: XRD spectra of hard deposit samples.

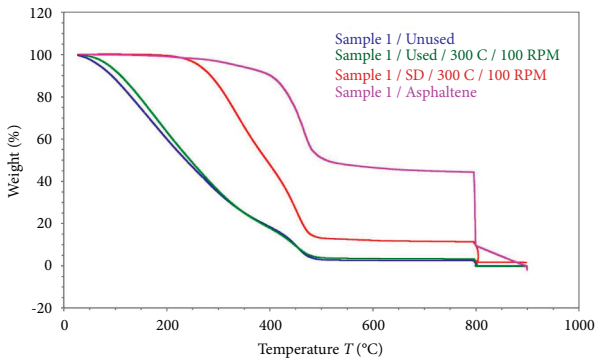

Figure 7: Thermal properties of crude oil, soft deposit, and C_7 asphaltenes at 300°C.

95% at this temperature. No weight loss was observed in the soft deposit sample up to 160°C. The weight loss in SD is ~14% and ~85% at temperatures up to 300 and 475°C, respectively. This indicates the presence of heavier material in the soft deposit which is potentially formed via chemical reactions of precursors transported from the bulk or in the crude sample near the coupon surface. The combustible component in the SD is ~9.7% compared to ~2.5% in the crude. Past works have reported this part of the deposit to contain trapped crude oil. Subsequently, a TGA analysis of fresh and used crude from the above test run was also carried out, the thermal behavior of which is also shown in Figure 7. It is observed that the crude oil before and after use loses appreciable weight (~96%) as the temperature is ramped up from 30 to 475°C. Figure 7 also shows the thermal history of C_7 asphaltenes extracted from the fresh crude sample. The nature of SD is also distinct from asphaltene.

3.4. Surface Morphology of Coupons. Figures 8(b) and 8(c) show the morphology of the hard deposits on the surface of a coupon (without scraping) at 275 and 300°C, respectively. The surface morphology of a clean coupon referred to as control is also shown in Figure 8(a) for reference purposes.

The SEM micrograph indicates the agglomeration of deposit structures on the coupon at both temperatures. The agglomeration results in terrace-like structures at 300°C. Elemental mapping of deposits on the surface at the two temperatures is shown in Figure 9. The presence of sulfur at 300°C is consistent with the XRD spectra obtained for this element at the same temperature.

An EDAX analysis indicated the presence of carbon, iron, sulfur, and oxygen. No sulfur was detected on the control surface. The composition of Fe and S in the deposit layer was greater than 45% at the two temperatures investigated.

The characterization of the hard and soft deposits presented in the preceding sections leads to the following observations:

(i) Both hard and soft deposits contribute to the fouling process. The results obtained in the present study align with the hypothesis of Atkins [46] who proposed that a fouling layer might comprise a porous or tarry layer and a hard crust layer.

(ii) The mechanism of fouling is largely corrosion-based at the temperatures investigated and driven by the formation of FeS on the surface. This agrees with the identification of more than 45 wt. % in total of Fe and S elements in the hard deposit.

(iii) The presence of iron and oxygen in the hard deposits is indicative of iron oxide forming on the surface, confirmed by a change in surface morphology and confirmed by the XRD spectra shown in Figure 6.

(iv) The nature of SD is different from crude and its effect on fouling must be accounted for when predicting the associated fouling mechanisms.

These observations are consistent with the findings of several laboratory studies made on crude oil corrosion [31, 40, 41]. These studies, however, do not emphasize the role of SD in the fouling phenomena. Sulfur is generally present in refinery streams such as H_2S, organosulfur (thiols, mercaptans, sulfides, benzothiophenes, polysulfides, etc.), and/or elemental sulfur. With sulfur being distributed across the carbon chain in these compounds, the C–S bonds break to form H_2S under appropriate conditions of temperature. In the absence of oxygen in the crude, naphthenic acid in crude oil reacts with iron on the coupon surface to iron naphthenate. Behranvand et al. [38] have shown carbon steel surfaces to be susceptible to naphthenic acid attack at temperatures above 260°C. These naphthenates decompose at higher temperatures into FeO which react with H_2S eventually forming FeS. In another mechanism, FeO which is thermodynamically unstable further forms Fe_2O_3/Fe_3O_4 and iron. The iron reacts with H_2S to form FeS. An XRF analysis of the hard deposit at 300°C showed the absence of FeO in the sample. An XRD analysis of hard deposits confirmed the presence of Fe_2O_3/Fe_3O_4. The formation of this sulfide layer leads to changes in surface properties like

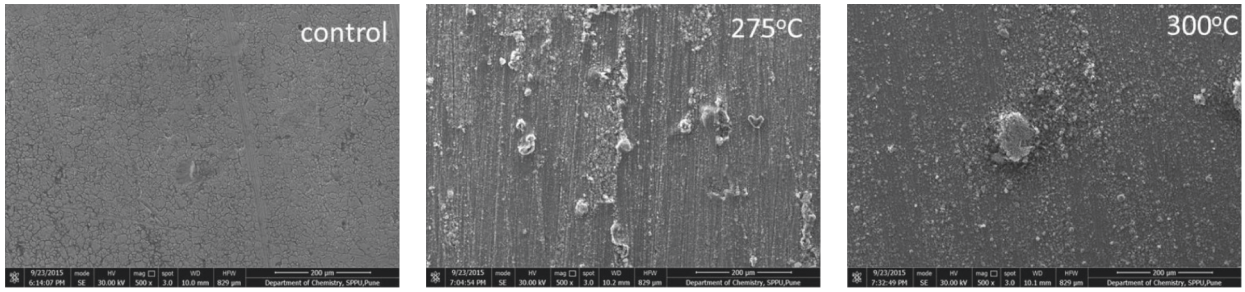

(a) (b) (c)

Figure 8: SEM images of coupon surface (a) without deposit (b) with deposit at 275°C (c) with deposit at 300°C.

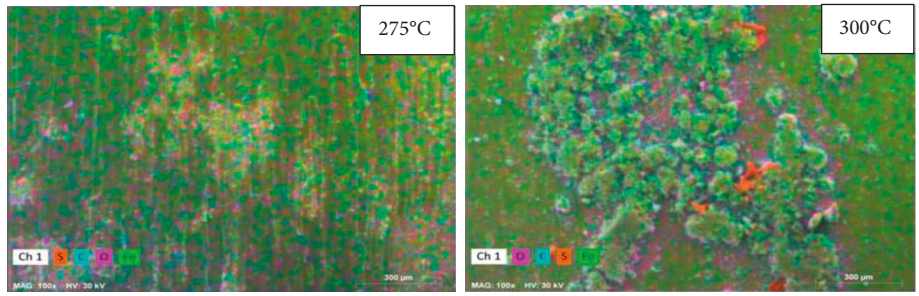

Figure 9: Elemental mapping on coupon surface with hard deposits at 275 and 300°C.

Table 5: Effect of temperature on the formation of hard and soft deposits.

Bulk temperature at 100 RPM (°C)	Hard deposit (mg)		Soft deposit (mg)	
	Coupon 1	Coupon 2	Coupon 1	Coupon 2
250	5.7	5.7	14.7	14.9
275	14.0	15.7	17.6	22.1
300	21.5	23.4	31.5	38.1

Table 6: Fouling potential of refinery streams based on the combination of bulk and surface temperature.

Bulk temperature	Surface temperature	Fouling potential	Nature of foulant deposit
High	High	High	Hard deposit
High	Low	Low	Soft deposit
Low	Low	Low	Soft deposit
Low	High	High	Hard deposit

interfacial tension, surface area, and surface roughness, which in turn promotes further fouling which is largely organic in nature and originates from the soft deposit adjacent to the sulfide layer.

3.5. Temperature Effect on the Formation of Hard and Soft Deposits. The influence of bulk temperature on the amount of hard and soft deposits formed on a coupon surface is discussed in this section. The results for three different bulk temperatures at 100 RPM are shown in Table 5. Both hard and soft deposit formation is found to increase with temperature.

The amount of hard deposits formed at 250°C is one order of magnitude lower than the amount of soft deposits formed at the same temperature. The order of magnitude, however, becomes comparable at 275 and 300°C. This can be attributed to an increase in the rate of formation of FeS on the coupon surface at these temperatures. The higher temperature also promotes chemical reactions in the soft deposit and subsequent conversion of soft deposits to hard deposits due to the change in surface characteristics. The reaction rate of the chemical species and adhesion in the soft deposits dominates the rate of formation of FeS at higher temperatures. Table 5 also shows the respective amounts of deposits formed on another coupon under the same conditions. The results obtained are consistent with the data obtained from the TGA analysis.

In practical systems at near-constant stream velocity, fouling will depend on a combination of bulk and surface temperatures, the effect of which based on the present investigation is summarized and shown in Table 6. The Table is

indicative and fouling will also be dependent on other factors like changes in stream velocity, oil composition, and MOC of the surface. The results obtained present an excellent case for adopting the test rig to characterize fouling associated with liquid refinery streams. Future work involves operating the rig at higher temperatures (greater than 330°C) and RPM values to characterize asphaltene-based fouling and investigate the role of stream velocity on foulant deposition rate.

3.6. Conclusions. The feasibility and potential of a custom-designed coupon test rig have been experimentally demonstrated to study fouling in refinery streams. The test rig facilitates the use of coupon strips of simple geometry instead of the normally adopted tubular and annular surfaces, which greatly enhances the ease of operation during experimentation. Using a limited amount of test samples, this versatile test rig enables understanding of the effects of varying bulk temperature (easier to measure against surface temperature) on the foulant deposition rate and subsequent collection of these deposits for further characterization using a consistent repeatable and reproducible analytical protocol. It facilitates easy estimation of fouling rates under specified operating conditions. Studies conducted using a representative refinery stream indicated FeS-based corrosion to be the primary cause of fouling at the temperature levels investigated. Foulant deposits on a coupon surface were found to be hard and soft in nature. The amount of hard and soft deposits formed is influenced by bulk temperature. The effect of the soft deposit must be accounted for when characterizing fouling. The rig can be used to predict fouling at temperatures greater than 300°C which is the scope of future work. The data obtained from this rig can be used in conjunction with and supplement the fouling know-how available from systems based on heat transfer studies, thus providing further understanding of related complex fouling phenomena.

Nomenclature

T: Temperature (°C)

Subscripts

b: Bulk
i: Inlet
o: Outlet
w: Wall.

Data Availability

The data used to support the findings of this study are included within the article.

Disclosure

Present Address of Krishnaswamy Ponnani is 15/151 (Old 7/383) Sreenivas, Sivan Kovil Street, Tharakkad, Palakkad, Kerala 678001, India.

Conflicts of Interest

The authors declare that they have no conflicts of interest or personal relationships that could have appeared to influence the work reported in this paper.

Acknowledgments

The authors would like to thank the Central Sophisticated Instrument Facility (CSIF) at BITS Pilani K K Birla Goa Campus, the Sophisticated Analytical Instrument Facility (SAIF) at Indian Institute of Technology (IIT), Bombay, and the Analytical Science and Technology (AS&T) Division at Aditya Birla Science and Technology Co., Pvt., Ltd. (ABSTC), Bombay, for extending analytical facilities and support during this work. Analytical support from the Sophisticated Instrumentation Centre for Applied Research and Testing (SICART) and characterization-related inputs provided by Mr. Yadnesh Kesari are also gratefully acknowledged. The authors also acknowledge the support received from Bharat Petroleum Corporation Limited (BPCL) Corporate R&D, in timely providing refinery samples which were subsequently utilized in this work. The financial support provided for this work by the Centre for High Technology (CHT)-Ministry of Petroleum and Natural Gas, India, is gratefully acknowledged.

References

[1] A. P. Watkinson, "Deposition from crude oils in heat exchangers," *Heat Transfer Engineering*, vol. 28, no. 3, pp. 177–184, 2007.

[2] E. M. Ishiyama, W. R. Paterson, and D. I. Wilson, "The effect of fouling on heat transfer, pressure drop, and throughput in refinery preheat trains: optimization of cleaning schedules," *Heat Transfer Engineering*, vol. 30, no. 10–11, pp. 805–814, 2009.

[3] E. Andersson, "Minimising refinery costs using spiral heat exchangers," *Petroleum Technology Quarterly*, vol. 13, no. 2, pp. 75–84, 2008.

[4] M. D. Khairansyah and T. R. Biyanto, "Economical aspect of heat exchanger cleaning affected by fouling," *The 1st International Seminar on Science and Technology*, vol. 2, no. 1, pp. 27-28, 2015.

[5] M. A. Gadalla, Z. Olujic, P. J. Jansens, M. Jobson, and R. Smith, "Reducing CO_2 emissions and energy consumption of heat-integrated distillation systems," *Environmental Science and Technology*, vol. 39, no. 17, pp. 6860–6870, 2005.

[6] F. Coletti and S. Macchietto, "Refinery pre-heat train network simulation undergoing fouling: assessment of energy efficiency and carbon emissions," *Heat Transfer Engineering*, vol. 32, no. 3–4, pp. 228–236, 2011.

[7] F. Coletti, B. D. Crittenden, and S. Macchietto, "Basic science of the fouling process," *Crude Oil Fouling*, pp. 23–50, Elsevier Inc, Amsterdam, Netherlands, 2015.

[8] S. I. Andersen and J. G. Speight, "Petroleum resins: separation, character, and role in petroleum," *Petroleum Science and Technology*, vol. 19, no. 1–2, pp. 1–34, 2001.

[9] N. Aske, H. Kallevik, and J. Sjöblom, "Determination of saturate, aromatic, resin, and asphaltenic (SARA) components in crude oils by means of infrared and near-infrared

spectroscopy," *Energy and Fuels*, vol. 15, no. 5, pp. 1304–1312, 2001.

[10] T. Fan and J. S. Buckley, "Rapid and accurate SARA analysis of medium gravity crude oils," *Energy and Fuels*, vol. 16, no. 6, pp. 1571–1575, 2002.

[11] G. Liu, K. Liao, W. Deng, and Y. Li, "Quantification of asphaltene content in viscous crude by K-ratio dual-wave length spectrophotometry," *Petroleum Science and Technology*, vol. 20, no. 1–2, pp. 43–48, 2002.

[12] J. Woods, J. Kung, D. Kingston, L. Kotlyar, B. Sparks, and T. Mccracken, "Canadian crudes: a comparative study of SARA fractions from a modified HPLC separation technique," *Oil & Gas Science and Technology*, vol. 63, no. 1, pp. 151–163, 2008.

[13] S. Akmaz, O. Iscan, M. A. Gurkaynak, and M. Yasar, "The structural characterization of saturate, aromatic, resin, and asphaltene fractions of Batiraman crude oil," *Petroleum Science and Technology*, vol. 29, no. 2, pp. 160–171, 2011.

[14] S. O. Honse, S. R. Ferreira, C. R. E. Mansur, E. F. Lucas, and G. González, "Separation and characterization of asphaltenic subfractions," *Quimica Nova*, vol. 35, no. 10, pp. 1991–1994, 2012.

[15] A. H. Mohammadi, A. Eslamimanesh, F. Gharagheizi, and D. Richon, "A novel method for evaluation of asphaltene precipitation titration data," *Chemical Engineering Science*, vol. 78, pp. 181–185, 2012.

[16] E. Keshmirizadeh, S. Shobeirian, and M. Memariani, "Determination of saturates, aromatics, resins and asphaltenes (SARA) fractions in Iran crude oil sample with chromatography methods: study of the geochemical parameters," *Journal of Applied Chemical Research*, vol. 7, pp. 15–24, 2013.

[17] M. K. Eyles and G. L. Wagner, "Method for determining fouling," U.S. Patent No. 4176544, 1979.

[18] P. E. Eaton, "Fouling test apparatus," U.S. Patent No. 4383438, 1983.

[19] P. E. Eaton, "Method and apparatus for conducting fouling tests," U.S. Patent No. 4910999, 1990.

[20] T. J. Clark, M. J. Hanagan, R. W. Cruse, V. A. Szalai, S. J. Rohman, and R. M. Mininni, "Method for passivating the inner surface by deposition of a ceramic coating of an apparatus subject to coking, apparatus prepared thereby, and method of utilizing apparatus prepared thereby," U.S. Patent No. 5208069, 1993.

[21] C. B. Panchal and Z. Mao, "High temperature fouling test unit," U.S. Patent No. 6062069, 2000.

[22] G. B. Brons, "Method and systems for predicting a need for introducing anti-fouling additives to a hydrocarbon stream to reduce fouling of crude hydrocarbon refinery components," U.S. Patent No. 9416325B2, 2016.

[23] W. C. Kuru and C. B. Panchal, "High-temperature orgnic-fluid fouling unit," Report, pp. 1–8, University of North Texas, Denton, TX, USA, 1997.

[24] M. Jamialahmadi, B. Soltani, H. Müller-Steinhagen, and D. Rashtchian, "Measurement and prediction of the rate of deposition of flocculated asphaltene particles from oil," *International Journal of Heat and Mass Transfer*, vol. 52, no. 19–20, pp. 4624–4634, 2009.

[25] Z. Fan, P. Rahimi, R. McGee, Q. Wen, and T. Alem, "Investigation of fouling mechanisms of a light crude oil using an alcor hot liquid process simulator," *Energy & Fuels*, vol. 24, no. 11, pp. 6110–6118, 2010.

[26] A. Young, S. Venditti, C. Berrueco et al., "Characterization of crude oils and their fouling deposits using a batch stirred cell system," *Heat Transfer Engineering*, vol. 32, no. 3–4, pp. 216–227, 2011.

[27] B. D. Crittenden, S. T. Kolaczkowski, T. Takemoto, and D. Z. Phillips, "Crude oil fouling in a pilot-scale parallel tube Apparatus," *Heat Transfer Engineering*, vol. 30, no. 10–11, pp. 777–785, 2009.

[28] A. D. Smith, "Analysis of fouling rate and propensity for eight crude oil samples in annular test section," in *Proceedings of the International Conference on Heat Exchanger Fouling and Cleaning*, pp. 1–8, Budapest, Hungary, 2013.

[29] Z. Tajudin, J. A. Martinez-Minuesa, E. Diaz-Bejarano et al., "Experiment analysis and baseline hydraulic characterisation of HiPOR, a high pressure crude oil fouling rig," *Chemical Engineering Transactions*, vol. 43, pp. 1405–1410, 2015.

[30] Y. Al Obaidi, M. Kozminski, and J. D. Ward, "Method and device for quantitative measurement of crude oil fouling deposits of several crude oils and blends at a higher temperature and the impact of antifoulant additives," *Energy & Fuels*, vol. 32, no. 6, pp. 6782–6787, 2018.

[31] W. Wang and A. P. Watkinson, "Iron sulphide and coke fouling from sour oils: review and initial experiments," in *Proceedings of the International Conference on Heat Exchanger Fouling and Cleaning IX*, pp. 23–30, Crete Island, Greece, 2011.

[32] M. S. Rafeen, M. F. Mohamed, M. Z. Mamot, N. A. Manan, A. Shafawi, and M. Ramasamy, "Crude oil fouling: PETRONAS refineries experience," *Heat Exchanger Fouling and Cleaning VII*, vol. RP5, pp. 8–12, 2007.

[33] D. A. Muñoz Pinto, S. M. Cuervo Camargo, M. Orozco Parra, D. Laverde, S. García Vergara, and C. Blanco Pinzon, "Formation of fouling deposits on a carbon steel surface from Colombian heavy crude oil under preheating conditions," *Journal of Physics: Conference Series*, vol. 687, no. 1, Article ID 012016, 2016.

[34] M. Srinivasan and A. P. Watkinson, "Fouling of some Canadian crude oils," *Heat Transfer Engineering*, vol. 26, no. 1, pp. 7–14, 2005.

[35] C. A. Bennett, R. S. Kistler, K. Nangia, W. Al-Ghawas, N. Al-Hajji, and A. Al-Jemaz, "Observation of an isokinetic temperature and compensation effect for high-temperature crude oil fouling," *Heat Transfer Engineering*, vol. 30, no. 10–11, pp. 794–804, 2009.

[36] Z. S. Saleh, R. Sheikholeslami, and A. P. Watkinson, "Fouling characteristics of a light Australian crude oil," *Heat Transfer Engineering*, vol. 26, no. 1, pp. 15–22, 2005.

[37] E. Diaz-Bejarano, E. Behranvand, F. Coletti, M. R. Mozdianfard, and S. Macchietto, "Organic and inorganic fouling in heat exchangers-industrial case study:analysis of fouling rate," *Industrial & Engineering Chemistry Research*, vol. 58, no. 1, pp. 228–246, 2018.

[38] E. Behranvand, M. R. Mozdianfard, E. Diaz-Bejarano, F. Coletti, P. Orzlowski, and S. Macchietto, "A comprehensive investigation of refinery preheaters foulant samples originated by heavy crude oil fractions as heating fluids," *Fuel*, vol. 224, pp. 529–536, 2018.

[39] R. A. Shank and T. R. Mccartney, "Characterization of crude oil fouling: defining the coke spectrum," *Heat Exchanger Fouling and Cleaning*, 2019.

[40] W. Wang and A. P. Watkinson, "Deposition from a sour heavy oil under incipient coking conditions: effect of surface materials and temperature," *Heat Transfer Engineering*, vol. 36, no. 7-8, pp. 623–631, 2015.

[41] W. Wang and A. P. Watkinson, "Deposition from a sour heavy oil under incipient coking conditions: wall shear effects

and mechanism," in *Proceedings of the International Conference on Heat Exchanger Fouling and Cleaning*, pp. 65–73, Enfield, Ireland, June 2015.

[42] P. Ramchandran, R. Sundar, G. Michael, and V. Jovancicevic, "Shear stress profile in a rotating cage," in *Proceedings of the International Conference on Corrosion CORCON*, pp. 26–28, Mumbai, India, September 2007.

[43] G. Brons, D. Brown, H. Joshi, T. Bruno, and T. M. Rudy, "Method for refinery foulant deposit charaterization," U.S. Patent No. 2006/0014296 A1, 2006.

[44] J. Chew, H. M. Joshi, S. G. Kazarian, M. Millan-Agorio, F. H. Tay, and S. Venditti, "Deposit characterization and measurements," *Crude Oil Fouling*, pp. 95–178, Elsevier Inc, Amsterdam, Netherlands, 2015.

[45] G. Radhika, R. Subadevi, K. Krishnaveni, W. R. Liu, and M. Sivakumar, "Synthesis and electrochemical performance of PEG-MnO_2–sulfur composites cathode materials for lithium–sulfur batteries," *Journal of Nanoscience and Nanotechnology*, vol. 18, no. 1, pp. 127–131, 2018.

[46] G. T. Atkins, "What to do about high coking rates," *Petroleum Chemical Engineering*, vol. 34, pp. 20–25, 1962.